

Optical Aharonov-Bohm Effect on Wigner Molecules in Type-II Semiconductor Quantum Dots

Rin Okuyama,* Mikio Eto, and Hiroyuki Hyuga
*Faculty of Science and Technology, Keio University,
3-14-1 Hiyoshi, Kohoku-ku, Yokohama 223-8522, Japan*
(Dated: November 5, 2018)

We theoretically examine the magnetoluminescence from a trion and a biexciton in a type-II semiconductor quantum dot, in which holes are confined inside the quantum dot and electrons are in a ring-shaped region surrounding the quantum dot. First, we show that two electrons in the trion and biexciton are strongly correlated to each other, forming a Wigner molecule: Since the relative motion of electrons is frozen, they behave as a composite particle whose mass and charge are twice those of a single electron. As a result, the energy of the trion and biexciton oscillates as a function of magnetic field with half the period of the single-electron Aharonov-Bohm oscillation. Next, we evaluate the photoluminescence. Both the peak position and peak height change discontinuously at the transition of the many-body ground state, implying a possible observation of the Wigner molecule by the optical experiment.

PACS numbers: 71.27.+a, 71.35.Ji, 73.21.-b, 78.55.-m, 78.67.Hc

I. INTRODUCTION

The electron-electron interaction in small rings is an important issue in mesoscopic physics.¹ This is exemplified by unsolved problems in the persistent current in normal metallic rings. When a magnetic flux penetrates the rings, the persistent current is induced by the Aharonov-Bohm (AB) effect in the thermal equilibrium state.^{2,3} The current observed in experiments⁴⁻⁸ is larger by at least 2 orders of magnitude than the theoretical prediction for noninteracting electrons.⁹⁻¹² Besides, the low-flux response is always diamagnetic in experimental results, whereas it is either diamagnetic or paramagnetic in theory. To resolve the discrepancies, the theory should take into account the electron-electron interaction.¹³ The attractive interaction as well as the repulsive one may play a role in explaining the diamagnetic response¹⁴ and the magnitude of the persistent current.¹⁵

The electron-hole interaction has also been examined in small rings fabricated on semiconductors. The AB effect on an exciton, consisting of an electron and a hole, was theoretically studied when the electron and hole are confined in small rings of different size.¹⁶⁻¹⁸ The AB effect becomes different in two situations, where the electron and hole move almost independently, or they tightly form an exciton. The AB effect on an exciton was observed through photoluminescence experiments, using quantum rings patterned on InGaAs/GaAs heterostructure¹⁹ and InAs/InP quantum tubes.²⁰ This is called the optical AB effect.

We focus on the type-II semiconductor quantum dots, such as InP/GaAs, ZnTe/ZnSe, and Ge/Si.²¹⁻²⁵ In these systems, holes are confined inside a quantum dot and electrons are in a ring-shaped region surrounding the quantum dot, as depicted in the inset of Fig. 1 (the roles of electron and hole are exchanged in the case of InP/GaAs). Since the motion of holes is almost frozen due to the strong confinement, the AB effect on the elec-

trons can be detected by the photoluminescence. For an exciton, we can adopt a simple model in which an electron is confined in a one-dimensional ring with a perpendicular magnetic field B . The Hamiltonian is given by

$$H = \frac{\hbar^2}{2m_e R^2} \left(\hat{L} - \frac{\Phi}{h/e} \right)^2, \quad (1)$$

where R is the radius of the ring, m_e is the effective mass of the electron, and \hat{L} is the angular momentum operator. $\Phi = \pi R^2 B$ is the magnetic flux penetrating the ring. The energy levels are shown in Fig. 1, as a function of magnetic flux Φ . The quantum number of the angular momentum \hat{L} , l , is indicated for the respective levels. With an increase in Φ , the ground state is changed from $l = 0$ to $l = 1$ at $\Phi = 0.5(h/e)$, from $l = 1$ to $l = 2$ at $\Phi = 1.5(h/e)$, and so on. As a result, the energy of the ground state oscillates as a function of Φ with the period of h/e . The magnetic-field dependence of the photoluminescence peak from an exciton is explained well by this simple model.^{18,21-25}

In the present paper, we theoretically examine the photoluminescence from a trion (two electrons and a hole) and a biexciton (two electrons and two holes) in type-II semiconductor quantum dots, in order to elucidate the correlation effect between electrons in a small ring. In our model, the holes are strongly confined in a harmonic potential, and thus their motion is almost frozen. This is the experimental situation of Ge/Si quantum dots.^{24,25} The electrons are in a quasi-one-dimensional ring-shaped potential, $V_e(r)$, shown in Fig. 2. First, we calculate the many-body states of a few electrons confined in $V_e(r)$ and show the formation of Wigner molecules owing to the strong correlation effect.²⁶⁻³⁰ In the Wigner molecules of N electrons, the electrons behave as a single particle whose mass and charge are N times of those of an electron. In consequence, the energy of the ground state oscillates with Φ by the period of $h/(Ne)$, the so-called frac-

tional AB effect.^{31–34} The formation of Wigner molecules is also seen for electrons in trions and biexcitons. Next, we examine the photoluminescence from the electron-hole complexes. We observe that the peak position and intensity of the photoluminescence, as a function of Φ , change discontinuously at the transition of the ground state. This implies a possible observation of the Wigner molecules by the optical experiment. We hope that our prediction will motivate the experimental study of trions and biexcitons in type-II quantum dots although there have not been such experiments until now.

We should make a comment on the cylindrical symmetry in our model as well as in the Hamiltonian in Eq. (1). As mentioned above, the peak position of the luminescence from an exciton can be explained using the Hamiltonian in Eq. (1), but the peak intensity cannot. For the optical recombination, the total angular momentum L of an electron and a hole must be zero because the final state is the vacuum with no electron or hole. Since the angular momentum of the hole is assumed to be zero in the ground state, the recombination is possible only at $\Phi \leq 0.5(h/e)$ where the angular momentum of the electron is $l = 0$.¹⁶ This contradicts the experimental results which observed a finite intensity at $\Phi > 0.5(h/e)$.^{21,23,25} This discrepancy could be resolved if the disorder of the system and finite temperature were taken into account.^{35–37} In our study we do not consider the disorder effect, which would modify our calculated results about the peak intensity of photoluminescence. On the other hand, our results about the peak position should not be changed qualitatively by the disorder. In particular, the discontinuous change of the peak position, which directly reflects the Wigner molecularization, can be experimentally observed although it is smeared to some extent. The discontinuous change of the peak intensity could be observed if well-shaped samples were fabricated.

The present paper is organized as follows. In Sec. II, we present our model and calculation method. We adopt the exact diagonalization method for the many-body states of electrons and holes. In Sec. III, we begin with the many-body states of a few electrons confined in the ring-shaped region. No holes are considered. We show the formation of Wigner molecules, reflecting the strong correlation effect. In Sec. IV, we calculate the many-body states of trions and biexcitons, in which two electrons form a Wigner molecule despite the presence of the holes. We evaluate the photoluminescence, using the many-body states obtained by the exact diagonalization method. Finally the conclusions are given in Sec. V.

II. MODEL AND CALCULATION METHOD

A. Effective-mass Hamiltonian

We consider a type-II semiconductor quantum dot of cylindrical symmetry in the xy plane. Holes are localized

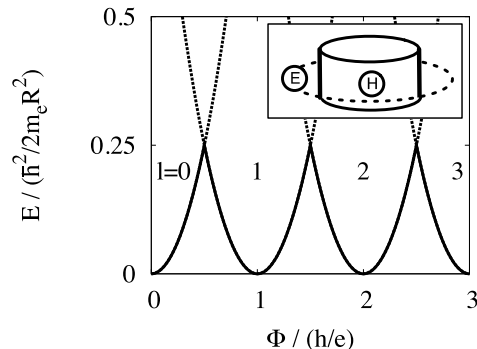


FIG. 1. Energy levels of an electron confined in a one-dimensional ring of radius R , as a function of perpendicular magnetic field B . $\Phi = \pi R^2 B$ is the magnetic flux penetrating the ring. The orbital angular momentum l is indicated for each energy level. Inset: A schematic drawing of the type-II semiconductor quantum dot, in which holes are confined inside the quantum dot and electrons are in a ring-shaped region surrounding the dot.

inside a quantum dot of disk shape, whereas electrons are confined in a ring-shaped region surrounding the dot. A magnetic field is applied perpendicularly to the quantum dot.

We adopt the effective-mass approximation, assuming that the radius of the quantum dot, $R \gtrsim 10$ nm, is much larger than the lattice constant a .^{21–25} For the holes, only the heavy-hole band (total angular momentum $j = 3/2$, $j_z = \pm 3/2$) is considered because the confinement in the z direction splits it from the light-hole band ($j = 3/2$, $j_z = \pm 1/2$).³⁸ The wave functions of the electron and hole are written as

$$\Psi_{e,\pm} = \psi_e(\mathbf{r}) u_c(\mathbf{r}) \chi_{\pm}, \quad (2)$$

$$\Psi_{h,\pm} = \psi_h(\mathbf{r}) u_{v,\mp}^*(\mathbf{r}) \chi_{\mp}, \quad (3)$$

respectively, where χ_{\pm} indicates the spin-up ($s_z = 1/2$) or -down ($s_z = -1/2$). $\psi_e(\mathbf{r})$ and $\psi_h(\mathbf{r})$ are envelope functions for electrons and holes, whereas $u_c(\mathbf{r})$ and $u_{v,\pm}(\mathbf{r})$ are the Bloch function of the conduction band (s wave) and valence band (orbital angular momentum $l_z = \pm 1$) at the Γ point, respectively.³⁹

The confinement potential for the holes is given by a harmonic potential

$$V_h(r) = \frac{1}{2} m_h \omega_h^2 r^2, \quad (4)$$

while that for the electrons is

$$V_e(r) = \frac{1}{2} m_e \omega_e^2 r^2 + V_0 \exp(-\alpha r^2), \quad (5)$$

where m_h and m_e are the effective masses of holes and electrons, respectively. The parameters ω_h , ω_e , V_0 , and α are chosen so that the radius of the electron confinement R at which $V_e(r)$ takes a minimum is eight times larger than the radius of hole confinement $\sqrt{\hbar/m_h \omega_h}$.

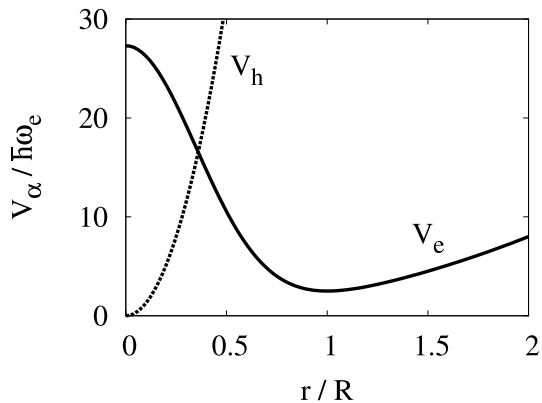


FIG. 2. The confinement potential for electrons, $V_e(r)$, and that for holes, $V_h(r)$, as a function of the radial coordinate r . R is the radius at which $V_e(r)$ takes a minimum.

This choice confirms the strong confinement of holes in a quantum dot, in accordance with the experimental situation.^{24,25} The confinement potentials $V_h(r)$ and $V_e(r)$ are depicted in Fig. 2.

The envelope functions $\psi_e(\mathbf{r})$ and $\psi_h(\mathbf{r})$ are determined from the effective-mass Hamiltonian. For N_e electrons and N_h holes, the Hamiltonian is given by

$$H = H_e + H_h + H_{e-h}, \quad (6)$$

$$H_e = \sum_{j=1}^{N_e} \left\{ \frac{1}{2m_e} \left[-i\hbar \frac{\partial}{\partial \mathbf{r}_{e,j}} + e\mathbf{A}(\mathbf{r}_{e,j}) \right]^2 + V_e(\mathbf{r}_{e,j}) \right\} + \sum_{1 \leq j < k \leq N_e} \frac{e^2}{4\pi\epsilon |\mathbf{r}_{e,j} - \mathbf{r}_{e,k}|}, \quad (7)$$

$$H_h = \sum_{j=1}^{N_h} \left\{ \frac{1}{2m_h} \left[-i\hbar \frac{\partial}{\partial \mathbf{r}_{h,j}} - e\mathbf{A}(\mathbf{r}_{h,j}) \right]^2 + V_h(\mathbf{r}_{h,j}) \right\} + \sum_{1 \leq j < k \leq N_h} \frac{e^2}{4\pi\epsilon |\mathbf{r}_{h,j} - \mathbf{r}_{h,k}|}, \quad (8)$$

$$H_{e-h} = \sum_{j=1}^{N_e} \sum_{k=1}^{N_h} \frac{-e^2}{4\pi\epsilon |\mathbf{r}_{e,j} - \mathbf{r}_{h,k}|}. \quad (9)$$

The magnetic field B is applied in the $-z$ direction: $\nabla \times \mathbf{A}(\mathbf{r}) = -B\mathbf{e}_z$. H_e (H_h) is the Hamiltonian for interacting electrons (holes), whereas H_{e-h} describes the electron-hole interaction. We assume that the dielectric constant ϵ is identical for electrons and holes. The spin Zeeman effect is neglected.

In H_{e-h} , the exchange-type interaction between an electron and a hole is disregarded for the following reason. For the wave functions in Eqs. (2) and (3), the matrix element of

$$\langle \Psi'_{e,\sigma} \Psi'_{h,-\sigma} | H_{e-h} | \Psi_{h,-\sigma} \Psi_{e,\sigma} \rangle = \int^{(3D)} d\mathbf{r}_1 d\mathbf{r}_2 \Psi'_{e,\sigma}{}^*(\mathbf{r}_1) \Psi'_{h,-\sigma}{}^*(\mathbf{r}_2) \frac{-e^2}{4\pi\epsilon |\mathbf{r}_1 - \mathbf{r}_2|} \Psi_{h,-\sigma}(\mathbf{r}_1) \Psi_{e,\sigma}(\mathbf{r}_2)$$

for $\sigma = \pm$,³⁹ involves the integral of $u_c^*(\mathbf{r}_1)u_{v,\sigma}(\mathbf{r}_1)$, which oscillates with the period of the lattice constant a . In consequence, the matrix element is smaller by the order of $(a/R)^2 \sim 10^{-4}$ than the exchange interaction between two electrons or that between two holes. Therefore we only consider the matrix elements of $\langle \Psi'_{e,\sigma} \Psi'_{h,\sigma'} | H_{e-h} | \Psi_{e,\sigma} \Psi_{h,\sigma'} \rangle$ for H_{e-h} :

$$\langle \Psi'_{e,\sigma} \Psi'_{h,\sigma'} | H_{e-h} | \Psi_{e,\sigma} \Psi_{h,\sigma'} \rangle = \int d\mathbf{r}_1 d\mathbf{r}_2 \psi_e'^*(\mathbf{r}_1) \psi_h'^*(\mathbf{r}_2) \frac{-e^2}{4\pi\epsilon |\mathbf{r}_1 - \mathbf{r}_2|} \psi_e(\mathbf{r}_1) \psi_h(\mathbf{r}_2)$$

after the integrations of $|u_c(\mathbf{r}_1)|^2$ and $|u_v(\mathbf{r}_2)|^2$ over the unit cell of the lattice.

The strength of the magnetic field is measured by the flux penetrating the ring of radius R , $\Phi = \pi R^2 B$. The ratio of the strength of the Coulomb potential to the kinetic energy is characterized by the parameter of R/a_B , where $a_B = 4\pi\epsilon\hbar^2/(m_e e^2)$ is the effective Bohr radius for electrons. We assume that $R/a_B \gtrsim 1$, considering the

experimental situations.²¹⁻²⁵

B. Exact diagonalization method

The many-body states of electrons and holes are calculated by the exact diagonalization method, taking full account of the Coulomb interaction. As a basis set, we

adopt the eigenfunctions of the one-body part of H_e in Eq. (7) for electrons and those of H_h in Eq. (8) for holes.⁴⁰ They are denoted by $\psi_{e,l,n}(\mathbf{r})$ and $\psi_{h,l,n}(\mathbf{r})$, respectively, with quantum number of orbital angular momentum ($l = 0, \pm 1, \pm 2, \dots$) and that of radial motion ($n = 1, 2, 3, \dots$).

Note that the effective-mass Hamiltonian in Eq. (6) has an axial symmetry in space and that the electron spins are decoupled from the hole spins. Therefore, the total orbital angular momentum L , total electron spin ($S_e, S_{e,z}$), and total hole spin ($S_h, S_{h,z}$) are good quantum numbers. The energy eigenvalues do not depend on $S_{e,z}$ and $S_{h,z}$. Hence we diagonalize the Hamiltonian in the subspace with given values of L , $S_{e,z}$, and $S_{h,z}$, the dimensions of which are less than 10^4 .⁴¹ The truncation of the Hamiltonian matrix leads to an inaccuracy of 0.1% for the total energy and of 1% for the intensity of the photoluminescence.

C. Photoluminescence

We evaluate the photoluminescence from a trion and a biexciton, using the many-body states obtained by the exact diagonalization method. We assume that the initial state is the ground state of the trion or biexciton.

When an electron with spin-up ($\Psi_{e,+}$) recombines with a hole with spin-down ($\Psi_{h,+}$), a right-circular photon is emitted. Similarly, when an electron with spin-down ($\Psi_{e,-}$) recombines with a hole with spin-up ($\Psi_{h,-}$), a left-circular photon is emitted. The recombination rate is evaluated by Fermi's golden rule with the dipole approximation.^{42,43} The interband dipole-moment operator is given by

$$\hat{d} = \sum_{l,n_1,n_2} \sum_{\sigma=\pm} d_{l,n_1,n_2} \hat{e}_{l,n_1,\sigma} \hat{h}_{-l,n_2,\sigma} + \text{h.c.}, \quad (10)$$

where $\hat{e}_{l,n,\sigma} [\hat{h}_{l,n,\sigma}]$ is an annihilation operator of an electron [a hole] in the state of $\psi_{e,l,n}\chi_\sigma$ [$\psi_{h,l,n}\chi_\sigma$] and

$$d_{l,n_1,n_2} = d_{vc} \int d\mathbf{r} \psi_{e,l,n_1}(\mathbf{r}) \psi_{h,-l,n_2}(\mathbf{r}), \quad (11)$$

$$d_{vc} = \left| \int_{\text{unit cell}}^{(3D)} d\mathbf{r} u_{v,\sigma}^*(\mathbf{r}) (-e\mathbf{r}) u_c(\mathbf{r}) \right|. \quad (12)$$

d_{vc} is independent of $\sigma = \pm$. The transition rate from the initial state $|\text{init}\rangle$ with energy E_{init} to the final state $|\text{fin}\rangle$ with energy E_{fin} is written as⁴⁴

$$I = \frac{4}{3} \frac{E^3}{4\pi\epsilon_0 \hbar^4 c^3} |\langle \text{fin} | \hat{d} | \text{init} \rangle|^2, \quad (13)$$

which is accompanied by the photon emission of energy $E = E_{\text{init}} - E_{\text{fin}} (\simeq E_{\text{gap}}$, band gap). Note that the total angular momentum L and the total spin $S_{e,z} + S_{h,z}$ should be conserved during the transition, as seen in Eq. (11). The intensity of the photoluminescence is evaluated by I , with E being replaced by E_{gap} .

III. WIGNER MOLECULES OF FEW ELECTRONS

We begin with the many-body states of a few electrons confined in a ring-shaped potential $V_e(r)$ in Eq. (5), to illustrate the Wigner molecularization. The number of electrons is $N_e = 1$ to 3. No holes are assumed in this section. The many-body states and energies are obtained using the exact diagonalization method for the Hamiltonian H_e in Eq. (7).

The calculated results of the energies are shown in Fig. 3 as a function of magnetic flux Φ , for (a) $N_e = 1$, (b) 2, and (c) 3. $R/a_B = 1$. The total angular momentum L is indicated for respective states. For one electron, the transition of the ground state takes place at $\Phi \simeq 0.5$ and 1.5 in units of h/e . The angular momentum increases by one at each transition. The Φ dependence of the energies is similar to that in Fig. 1 for an electron in a one-dimensional ring although the diamagnetic shift of the energies is seen in Fig. 3(a). Therefore, the energy of the ground state oscillates with the period of approximately h/e , reflecting the one-dimensional motion along the ring.

Note that the state of L in Fig. 3(a) corresponds to $\psi_{e,L,1}$ introduced in Sec. II.B. The energies of the excited states in the radial motion, $\psi_{e,L,n}$ ($n \geq 2$), are larger by more than $2\hbar\omega_e$ than those of the lowest states. In the low-lying states of two and three electrons, shown in Figs. 3(b) and 3(c), the weight of $\psi_{e,L,n}$ ($n \geq 2$) is of the order of 10^{-3} . Therefore, electrons possess a one-dimensional nature in our model.

In Figs. 3(b) and 3(c), we observe the change of the ground state for two and three electrons. If the diamagnetic shift is disregarded, the energy of the ground state oscillates quasiperiodically with the period of $h/(2e)$ for two electrons and $h/(3e)$ for three electrons. This implies the formation of Wigner molecules as explained below.

In order to elucidate the correlation effect, we examine many-body states for two electrons with changing R/a_B . Figure 4 shows low-lying energies in the case of $R/a_B = 0.01, 0.1, 1, \text{ and } 10$. When the Coulomb interaction is very weak ($R/a_B = 0.01$), two electrons occupy the lowest orbital shown in Fig. 3(a) in the ground state. Consequently, the total angular momentum is always even and the total spin is a singlet. As the strength of the Coulomb interaction increases with R/a_B , the exchange interaction lowers the energy of the spin-triplet states with $L = 1$ and 3. For $R/a_B \gtrsim 1$, spin-singlet and -triplet states appear alternatively as Φ increases by approximately $h/(2e)$. Thus the fractional period of the energy oscillation is ascribable to the strong correlation effect. Note that the period of the energy oscillation in the case of $R/a_B = 10$ is slightly shorter than that of $R/a_B = 1$. This is because the Coulomb repulsion between electrons increases the expectation value of the electron radius.

To examine the correlation effect further, we calculate

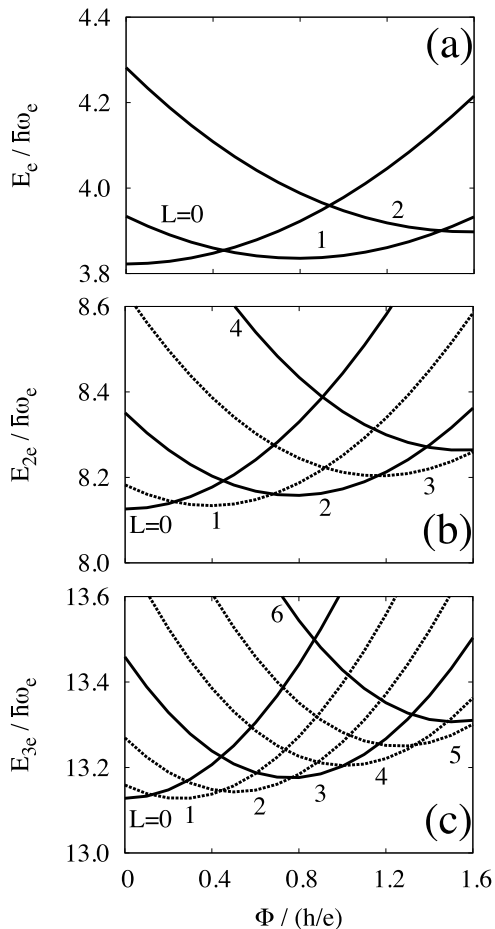


FIG. 3. Low-lying energies for (a) one, (b) two, and (c) three electrons confined in a ring-shaped potential, $V_e(r)$, as a function of the magnetic flux Φ . The radius R at which $V_e(r)$ takes a minimum equals the effective Bohr radius a_B . $\Phi = \pi R^2 B$. Solid and broken lines indicate spin-singlet and -triplet states, respectively, in (b), and spin-quartet and -doublet states in (c).

the two-body density

$$\rho(\mathbf{r}|\mathbf{r}_0) = \frac{1}{2} \sum_{\sigma, \sigma_0} \langle \hat{\psi}_{e, \sigma}^\dagger(\mathbf{r}) \hat{\psi}_{e, \sigma_0}^\dagger(\mathbf{r}_0) \hat{\psi}_{e, \sigma_0}(\mathbf{r}_0) \hat{\psi}_{e, \sigma}(\mathbf{r}) \rangle, \quad (14)$$

where $\hat{\psi}_{e, \sigma}(\mathbf{r})$ and $\hat{\psi}_{e, \sigma}^\dagger(\mathbf{r})$ are the field operators of electron with spin σ . Figure 5 shows $\rho(\mathbf{r}|\mathbf{r}_0)$ for two electrons in the ground state at the magnetic flux $\Phi = 0$. \mathbf{r}_0 is fixed at the position indicated by an open circle. R/a_B is changed in the same way as in Fig. 4. For $R/a_B \gtrsim 1$, two electrons maximize their distance by being localized at the other side of each other in the ring. This clearly indicates the formation of the Wigner molecule. Since the relative motion is frozen, the two electrons behave as a composite particle whose mass and charge are twice those of an electron. In consequence the ground-state energy oscillates with Φ by the period of $h/(2e)$.

For three electrons, a similar formation of the Wigner

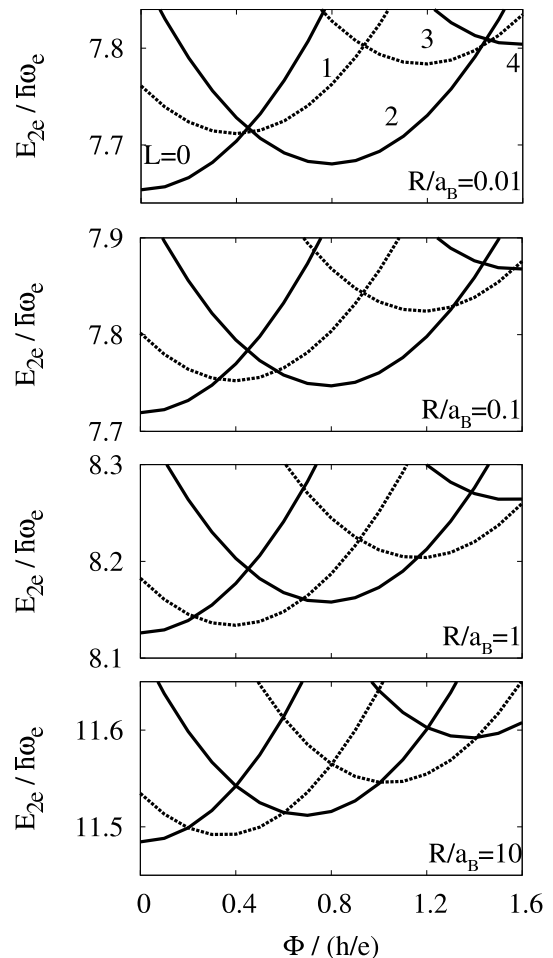


FIG. 4. Low-lying energies for two electrons confined in a ring-shaped potential, $V_e(r)$, as a function of the magnetic flux Φ . $R/a_B = 0.01, 0.1, 1, \text{ and } 10$, where R is the radius at which $V_e(r)$ takes a minimum and a_B is the effective Bohr radius. $\Phi = \pi R^2 B$. Solid and broken lines indicate spin-singlet and -triplet states, respectively.

molecule is observed for $R/a_B \gtrsim 1$. Figure 6 shows the two-body density for three electrons in the ground state at $\Phi = 0$. The electrons are localized around apices of an equilateral triangle in the ring. The molecularization explains the energy oscillation with the period of $h/(3e)$ in Fig. 3(c).

We make a comment on the total spin S of the ground state. The spin S changes with the total angular momentum L at the transition of the ground state shown in Fig. 3. For two electrons, as we mentioned above, $S = 0$ ($S = 1$) when L is an even (odd). For three electrons, $S = 3/2$ if L is a multiple of 3 and $S = 1/2$ otherwise. This was explained by the N_e -fold rotational symmetry of N_e -electron configuration in the Wigner molecule.^{45–47}

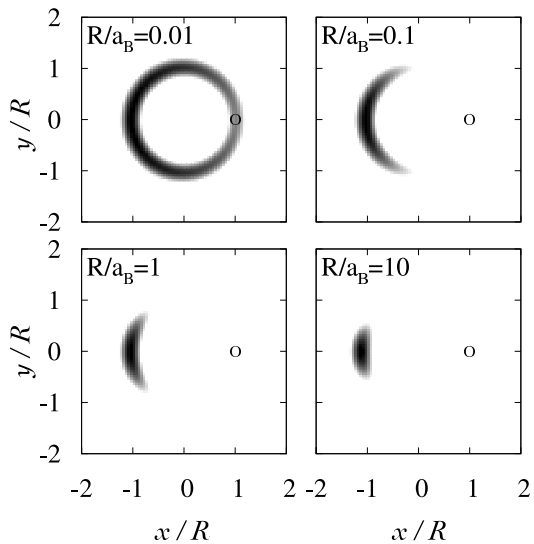


FIG. 5. Gray scale plots of the two-body density for two electrons confined in a ring-shaped potential, $V_e(r)$. The magnetic field is $B = 0$. $R/a_B = 0.01, 0.1, 1$, and 10 , where R is the radius at which $V_e(r)$ takes a minimum and a_B is the effective Bohr radius. One electron is fixed at the point indicated by an open circle.

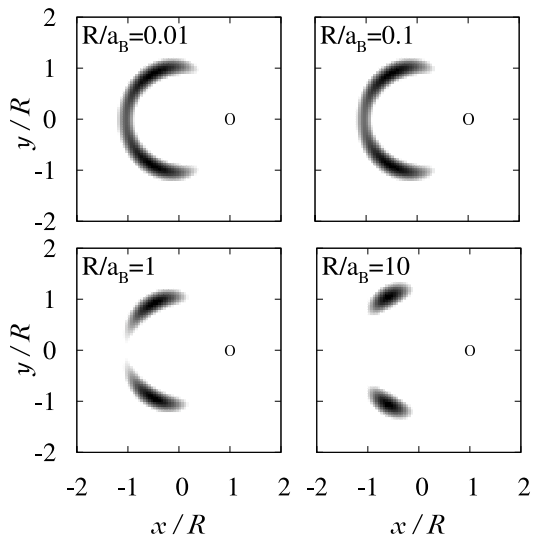


FIG. 6. Gray scale plots of the two-body density for three electrons confined in a ring-shaped potential, $V_e(r)$. The magnetic field is $B = 0$. $R/a_B = 0.01, 0.1, 1$, and 10 , where R is the radius at which $V_e(r)$ takes a minimum and a_B is the effective Bohr radius. One electron is fixed at the point indicated by an open circle.

IV. ELECTRON-HOLE COMPLEXES AND OPTICAL RESPONSE

In this section, we examine the many-body states of electron-hole complexes, that is, exciton, trion, and biexciton. We consider the case of $R/a_B = 1$, in which two electrons form a Wigner molecule in the cases of trion

and biexciton. First, the low-lying states are analyzed as a function of magnetic flux Φ . Then the photoluminescence is examined from the ground state in trion and biexciton.

A. Low-lying states

Figure 7 shows the low-lying energies for (a) exciton, (b) trion, and (c) biexciton, as a function of magnetic flux Φ . For an exciton in Fig. 7(a), the angular momentum of the ground state changes at $\Phi \approx 0.5(h/e)$ and $1.5(h/e)$, which is qualitatively the same as in Fig. 3(a) for an electron confined in $V_e(r)$. This is because the hole occupies the lowest state with angular momentum $l = 0$ and is insensitive to the magnetic field.

For the trion and biexciton in Figs. 7(b) and 7(c), the ground state changes in a similar manner to that for two electrons confined in $V_e(r)$ [Fig. 3(b)]. A hole or two holes occupy the lowest state with angular momentum $l = 0$, which is hardly influenced by the magnetic field. Two electrons in a trion and a biexciton form a Wigner molecule, which is reflected by the energy oscillation with the period of $h/(2e)$.

Precisely speaking, the magnetic flux Φ at the transition of the ground state is slightly shifted to the larger values for the trion [Fig. 7(b)] and biexciton [Fig. 7(c)], compared with the two-electron case [Fig. 3(b)]. This is because one hole or two holes inside the quantum dot decrease the effective radius of electrons. Although the screening by the holes should weaken the electron-electron interaction, its effect is invisible: The screening effect on the Wigner molecule is negligible unless it is so large as to break the molecule.

B. Photoluminescence

Now we discuss the photoluminescence from the electron-hole complexes. Figure 8 shows the Φ dependence of (a) peak position and (b) intensity of the photoluminescence from an exciton. The peak position coincides with the ground-state energy shown in Fig. 7 because the final state is the vacuum. The optical recombination of the exciton is possible when the angular momentum of the electron is $l = 0$ since that of the hole is always $l = 0$. In consequence the exciton gets dark after the first transition of the electronic state at $\Phi \approx 0.5(h/e)$, as mentioned in Sec. I.

In the photoluminescence from a trion, there are two electrons and a hole in the initial state, and an electron in the final state. If the ground state of the trion has the angular momentum L , it changes to a one-electron state of $\psi_{e,L,n}$ ($n = 1, 2, \dots$). The transition to $\psi_{e,L,1}$ is dominant because the weight of $\psi_{e,L,n}$ ($n \geq 2$) is very small in the ground state. The transition to the higher states is neglected since the intensity is 10^{-3} times as small as that of the dominant transition.

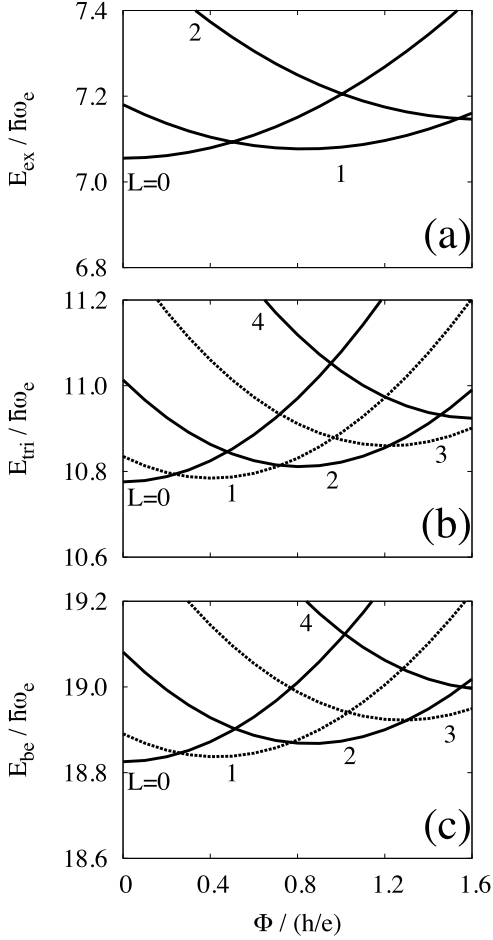


FIG. 7. Low-lying energies for (a) exciton, (b) trion, and (c) biexciton, as a function of the magnetic flux Φ . The radius R , at which $V_e(r)$ takes a minimum, equals the effective Bohr radius a_B . $\Phi = \pi R^2 B$. In (b) and (c), solid and broken lines indicate the spin states of electrons: spin-singlet and -triplet states, respectively.

The position and intensity of the dominant peak from a trion are shown in Fig. 9, as a function of magnetic flux Φ . The peak position increases with an increase in Φ , and suddenly drops when the angular momentum

L is changed in the ground state of the trion. At the transition of L , the final state is changed. As a result, the energy of the final state, E_e , is discontinuously changed, whereas the energy of the initial state, E_{2e} , is continuous as shown in Fig. 7(b).

As seen in Fig. 9(b), the intensity of the photoluminescence from a trion shows a plateau structure as a function of Φ : While the angular momentum L is not changed in the ground state, the intensity is almost constant. At the transition of L , the intensity decreases abruptly. The height of the plateaus indicates a ratio of 4 : 3 : 1 : 0 approximately.

The simple ratio of the intensity is explained in the following. The strongly correlated two-electron states can

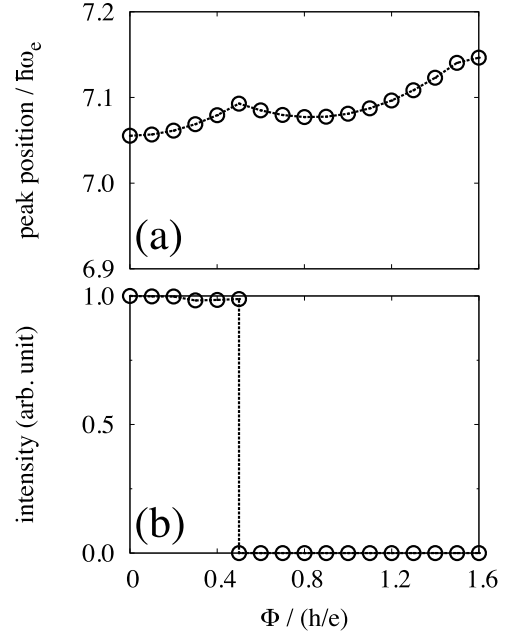


FIG. 8. (a) The peak position and (b) intensity of the photoluminescence from an exciton, as a function of the magnetic flux Φ . The radius R , at which $V_e(r)$ takes a minimum, equals the effective Bohr radius a_B . $\Phi = \pi R^2 B$.

be approximated by a few electronic configurations:

$$|L = 0\rangle = \left[\sqrt{\frac{2}{3}} \hat{e}_{0,+}^\dagger \hat{e}_{0,-}^\dagger - \sqrt{\frac{1}{6}} (\hat{e}_{1,+}^\dagger \hat{e}_{1,-}^\dagger - \hat{e}_{1,-}^\dagger \hat{e}_{1,+}^\dagger) \right] |0\rangle, \quad (15)$$

$$|L = 1\rangle = \frac{1}{\sqrt{2}} (\hat{e}_{0,+}^\dagger \hat{e}_{1,-}^\dagger + \hat{e}_{0,-}^\dagger \hat{e}_{1,+}^\dagger) |0\rangle, \quad (16)$$

$$|L = 2\rangle = \left[\sqrt{\frac{2}{3}} \hat{e}_{1,+}^\dagger \hat{e}_{1,-}^\dagger - \sqrt{\frac{1}{6}} (\hat{e}_{2,+}^\dagger \hat{e}_{0,-}^\dagger - \hat{e}_{2,-}^\dagger \hat{e}_{0,+}^\dagger) \right] |0\rangle, \quad (17)$$

where $\hat{e}_{l,\sigma}^\dagger$ is the creation operator of an electron in state

$\psi_{e,l,1}\chi_\sigma$ (see the Appendix). These expressions are an

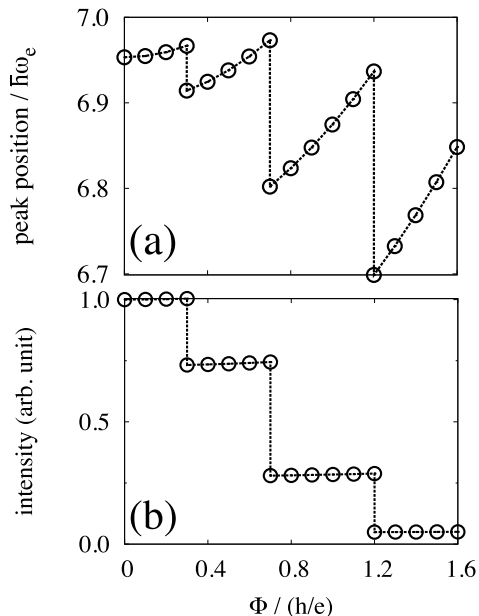


FIG. 9. (a) The peak position and (b) intensity of the photoluminescence from a trion, as a function of the magnetic flux Φ . The radius R , at which $V_e(r)$ takes a minimum, equals the effective Bohr radius a_B . $\Phi = \pi R^2 B$.

extension of the Heitler-London wave function for two electrons in a hydrogen molecule.⁴⁸ From the wave functions in Eqs. (15)–(17), we obtain the intensity ratio of 4 : 3 : 1 : 0, as explained in the Appendix.

Finally, we present the photoluminescence from a biexciton in Fig. 10. In this case, the final state is an excitonic state of the same angular momentum as the ground state of the biexciton. The Φ dependence of the peak position and intensity is qualitatively the same as that for the photoluminescence from a trion.

V. CONCLUSIONS

We have examined the magnetoluminescence from a trion and a biexciton in a type-II semiconductor quantum dot, in which holes are confined inside the quantum dot and electrons are in a ring-shaped region surrounding the quantum dot. First, we have calculated the many-body states by the exact diagonalization method. We have shown that the two electrons in trions and biexcitons form a Wigner molecule, reflecting a large correlation effect. The electrons behave as a composite particle whose mass and charge are twice those of a single electron. In consequence, the ground-state energy of the trion and biexciton oscillates as a function of magnetic flux Φ with a period of approximately $h/(2e)$. Next, we have evaluated the photoluminescence from the electron-hole complexes as a function of Φ . Both the peak position and peak intensity of the photoluminescence change dis-

continuously at the transition of the ground state. This

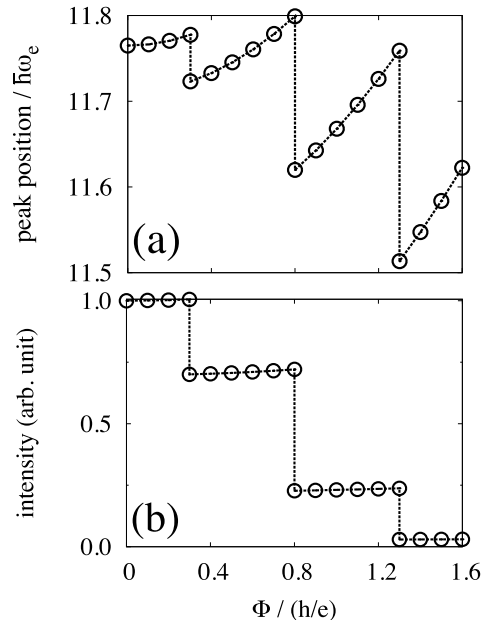


FIG. 10. (a) The peak position and (b) intensity of the photoluminescence from a biexciton, as a function of the magnetic flux Φ . The radius R , at which $V_e(r)$ takes a minimum, equals the effective Bohr radius a_B . $\Phi = \pi R^2 B$.

indicates a possible observation of Wigner molecules by optical experiment.

ACKNOWLEDGMENTS

The authors acknowledge fruitful discussion with K. M. Itoh, S. Miyamoto, and T. Ishikawa. This work was partly supported by a Grant-in-Aid for Scientific Research from the Japan Society for the Promotion of Science, and Graduate School Doctoral Student Aid Program from Keio University.

APPENDIX: APPROXIMATE WAVE FUNCTIONS OF TWO ELECTRONS IN RING

In a trion and a biexciton, two electrons are strongly correlated to each other, forming a Wigner molecule. In this appendix, we present a simple wave function to describe the two-electron state, neglecting the hole state. Using the wave function, we derive an intensity ratio of the photoluminescence shown in Figs. 9(b) and 10(b).

We construct a wave function by a few electronic configurations in which electrons occupy the lowest states in the radial motion, $\psi_{e,l,1}\chi_\sigma$. In general, $\psi_{e,l,n}$ is written as

$$\psi_{e,l,n}(\mathbf{r}) = R_{e,l,n}(r)e^{il\theta}, \quad (\text{A1})$$

where $R_{e,l,n}$ is determined by the equation

$$\left\{ \frac{\hbar^2}{2m_e} \left[-\frac{\partial^2}{\partial r^2} - \frac{1}{r} \frac{\partial}{\partial r} + \left(\frac{l}{r} - \frac{eBr}{2\hbar} \right)^2 \right] + V_e(r) \right\} R_{e,l,n} = \varepsilon_{e,l,n} R_{e,l,n}, \quad (\text{A2})$$

with $\varepsilon_{e,l,n}$ being the energy eigenvalue for the one-electron state. Since the electron is confined around $r = R$ by $V_e(r)$, both the centrifugal potential, $\hbar^2 l^2 / (2m_e r^2)$, and diamagnetic term, $(eBr)^2 / (8m_e)$, are ineffective. Hence, (i) we replace $R_{e,l,1}$ by $R_{e,1}$, disregarding its l dependence hereafter. (ii) The B dependence of $R_{e,1}$ is small. This explains the plateau structure of photoluminescence intensity, shown in Figs. 9(b) and 10(b), in which the intensity is almost constant as long as the angular momentum l does not change.

Let us begin with the lowest state with the total angular momentum $L = 0$. Without the Coulomb interaction, the lowest state is $\hat{e}_{0,+}^\dagger \hat{e}_{0,-}^\dagger |0\rangle$, where $\hat{e}_{l,\sigma}^\dagger$ is the creation operator of state $\psi_{e,l,1} \chi_\sigma$. The total spin is a singlet. The wave function becomes

$$\langle \mathbf{r}_1, \mathbf{r}_2 | \hat{e}_{0,+}^\dagger \hat{e}_{0,-}^\dagger |0\rangle = R_{e,1}(r_1) R_{e,1}(r_2) \frac{\chi_+(1)\chi_-(2) - \chi_-(1)\chi_+(2)}{\sqrt{2}}.$$

This has a finite value at $\theta_1 = \theta_2$ since no correlation effect is taken into account. We mix the second lowest state with $L = 0$, $(\hat{e}_{1,+}^\dagger \hat{e}_{-1,-}^\dagger - \hat{e}_{1,-}^\dagger \hat{e}_{-1,+}^\dagger) |0\rangle / \sqrt{2}$, as

$$|L = 0\rangle = \left[\sqrt{\frac{2}{3}} \hat{e}_{0,+}^\dagger \hat{e}_{0,-}^\dagger - \sqrt{\frac{1}{6}} (\hat{e}_{1,+}^\dagger \hat{e}_{-1,-}^\dagger - \hat{e}_{1,-}^\dagger \hat{e}_{-1,+}^\dagger) \right] |0\rangle. \quad (\text{A3})$$

Then its wave function is given by

$$\langle \mathbf{r}_1, \mathbf{r}_2 | L = 0\rangle = R_{e,1}(r_1) R_{e,1}(r_2) \frac{1 - \cos(\theta_1 - \theta_2)}{\sqrt{3/2}} \frac{\chi_+(1)\chi_-(2) - \chi_-(1)\chi_+(2)}{\sqrt{2}},$$

which vanishes at $\theta_1 = \theta_2$. Thus this is an appropriate state to describe the strongly correlated electrons in the Wigner molecule.

We proceed to the lowest state with $L = 1$. In the absence of Coulomb interaction, it is

$$|L = 1\rangle = \frac{1}{\sqrt{2}} (\hat{e}_{0,+}^\dagger \hat{e}_{1,-}^\dagger + \hat{e}_{0,-}^\dagger \hat{e}_{1,+}^\dagger) |0\rangle. \quad (\text{A4})$$

The total spin is a triplet. The orbital part of the wave function is

$$R_{e,1}(r_1) R_{e,1}(r_2) \frac{e^{i\theta_1} - e^{i\theta_2}}{2},$$

the amplitude of which is zero at $\theta_1 = \theta_2$. In the spin-triplet states, the exchange correlation reduces the Coulomb energy between electrons. Hence we adopt the state in Eq. (A4) as an approximate state for the Wigner molecule.

For the state with $L = 2$, we mix two electronic configurations, $\hat{e}_{1,+}^\dagger \hat{e}_{1,-}^\dagger |0\rangle$ and $(\hat{e}_{2,-}^\dagger \hat{e}_{0,-}^\dagger - \hat{e}_{2,+}^\dagger \hat{e}_{0,+}^\dagger) |0\rangle / \sqrt{2}$, in such a way that the wave function vanishes at $\theta_1 = \theta_2$. We obtain

$$|L = 2\rangle = \left[\sqrt{\frac{2}{3}} \hat{e}_{1,+}^\dagger \hat{e}_{1,-}^\dagger - \sqrt{\frac{1}{6}} (\hat{e}_{2,-}^\dagger \hat{e}_{0,-}^\dagger - \hat{e}_{2,+}^\dagger \hat{e}_{0,+}^\dagger) \right] |0\rangle. \quad (\text{A5})$$

The intensity of the photoluminescence from the states in Eqs. (A3)–(A5) is evaluated using Eq. (13). The hole

state is $\hat{h}_{0,+}^\dagger |0\rangle$ or $\hat{h}_{0,-}^\dagger |0\rangle$ in trion and $\hat{h}_{0,+}^\dagger \hat{h}_{0,-}^\dagger |0\rangle$ in biexciton, where $\hat{h}_{0,\sigma}^\dagger$ is the creation operator of $\psi_{h,0,1} \chi_{-\sigma} \equiv R_{h,1}(r) \chi_{-\sigma}$. From $|L = 0\rangle$, $|L = 1\rangle$, and $|L = 2\rangle$, the intensity is given by $(2/3)I_0$, $(1/2)I_0$, and $(1/6)I_0$, respectively, for the trion (they are twice for the biexciton). Here,

$$I_0 = \frac{4}{3} \frac{E_{\text{gap}}^3}{4\pi\epsilon_0 \hbar^4 c^3} \left| d_{\text{vc}} \int 2\pi r dr R_{e,1}(r) R_{h,1}(r) \right|^2, \quad (\text{A6})$$

where E_{gap} is the band gap and d_{vc} is given by Eq. (12).

The lowest states with $L > 2$ do not include the one-electron state with $l = 0$ ($\psi_{e,0,1} \chi_\sigma$) in our approximation. As a result, the intensity of the photoluminescence becomes zero. In conclusion, the ratio of the intensity is

$$I(L = 0) : I(L = 1) : I(L = 2) : I(L > 2) = 4 : 3 : 1 : 0. \quad (\text{A7})$$

- * rokuyama@rk.phys.keio.ac.jp
- ¹ S. Viefers, P. Koskinen, P. S. Deo, and M. Manninen, *Physica E* **21**, 1 (2004).
 - ² L. Gunther and Y. Imry, *Solid State Communications* **7**, 1391 (1969).
 - ³ M. Büttiker, Y. Imry, and R. Landauer, *Phys. Lett. A* **96**, 365 (1983).
 - ⁴ L. P. Lévy, G. Dolan, J. Dunsmuir, and H. Bouchiat, *Phys. Rev. Lett.* **64**, 2074 (1990).
 - ⁵ R. Deblock, R. Bel, B. Reulet, H. Bouchiat, and D. Mailly, *Phys. Rev. Lett.* **89**, 206803 (2002).
 - ⁶ E. M. Q. Jariwala, P. Mohanty, M. B. Ketchen, and R. A. Webb, *Phys. Rev. Lett.* **86**, 1594 (2001).
 - ⁷ H. Bluhm, N. C. Koshnick, J. A. Bert, M. E. Huber, and K. A. Moler, *Phys. Rev. Lett.* **102**, 136802 (2009).
 - ⁸ A. C. Bleszynski-Jayich, W. E. Shanks, B. Peaudecerf, E. Ginossar, F. von Oppen, L. Glazman, and J. G. E. Harris, *Science* **326**, 272 (2009).
 - ⁹ H.-F. Cheung, E. K. Riedel, and Y. Gefen, *Phys. Rev. Lett.* **62**, 587 (1989).
 - ¹⁰ O. Entin-Wohlman and Y. Gefen, *Europhys. Lett.* **8**, 477 (1989).
 - ¹¹ B. L. Altshuler, Y. Gefen, and Y. Imry, *Phys. Rev. Lett.* **66**, 88 (1991).
 - ¹² E. K. Riedel and F. von Oppen, *Phys. Rev. B* **47**, 15449 (1993).
 - ¹³ V. Ambegaokar and U. Eckern, *Phys. Rev. Lett.* **65**, 381 (1990).
 - ¹⁴ V. Ambegaokar and U. Eckern, *Europhys. Lett.* **13**, 733 (1990).
 - ¹⁵ H. Bary-Soroker, O. Entin-Wohlman, and Y. Imry, *Phys. Rev. Lett.* **101**, 057001 (2008).
 - ¹⁶ A. B. Kalameitsev, V. M. Kovalev, and A. O. Govorov, *JETP Lett.* **68**, 669 (1998).
 - ¹⁷ K. L. Janssens, B. Partoens, and F. M. Peeters, *Phys. Rev. B* **64**, 155324 (2001).
 - ¹⁸ A. O. Govorov, S. E. Ulloa, K. Karrai, and R. J. Warburton, *Phys. Rev. B* **66**, 081309 (2002).
 - ¹⁹ M. Bayer, M. Korkusinski, P. Hawrylak, T. Gutbrod, M. Michel, and A. Forchel, *Phys. Rev. Lett.* **90**, 186801 (2003).
 - ²⁰ K. Tsumura, S. Nomura, P. Mohan, J. Motohisa, and T. Fukui, *Jpn. J. Appl. Phys.* **46**, L440 (2007).
 - ²¹ E. Ribeiro, A. O. Govorov, W. Carvalho, and G. Medeiros-Ribeiro, *Phys. Rev. Lett.* **92**, 126402 (2004).
 - ²² I. L. Kuskovsky, W. MacDonald, A. O. Govorov, L. Muroukh, X. Wei, M. C. Tamargo, M. Tadic, and F. M. Peeters, *Phys. Rev. B* **76**, 035342 (2007).
 - ²³ I. R. Sellers, V. R. Whiteside, I. L. Kuskovsky, A. O. Govorov, and B. D. McCombe, *Phys. Rev. Lett.* **100**, 136405 (2008).
 - ²⁴ I. R. Sellers, V. R. Whiteside, A. O. Govorov, W. C. Fan, W.-C. Chou, I. Khan, A. Petrou, and B. D. McCombe, *Phys. Rev. B* **77**, 241302 (2008).
 - ²⁵ S. Miyamoto, O. Moutanabbir, T. Ishikawa, M. Eto, E. E. Haller, K. Sawano, Y. Shiraki, and K. M. Itoh, *Phys. Rev. B* **82**, 073306 (2010).
 - ²⁶ F. Bolton and U. Rössler, *Superlatt. and Microstructures* **13**, 139 (1993).
 - ²⁷ P. A. Maksym, *Phys. Rev. B* **53**, 10871 (1996).
 - ²⁸ M. Dineykhon and R. G. Nazmitdinov, *Phys. Rev. B* **55**, 13707 (1997).
 - ²⁹ C. Yannouleas and U. Landman, *Phys. Rev. Lett.* **85**, 1726 (2000).
 - ³⁰ M. Manninen, M. Koskinen, S. M. Reimann, and B. Mottelson, *Eur. Phys. J. D* **16**, 381 (2001).
 - ³¹ F. V. Kusmartsev, *J. Phys. Cond. Matt.* **3**, 3199 (1991).
 - ³² N. Yu and M. Fowler, *Phys. Rev. B* **45**, 11795 (1992).
 - ³³ F. V. Kusmartsev, J. F. Weisz, R. Kishore, and M. Takahashi, *Phys. Rev. B* **49**, 16234 (1994).
 - ³⁴ K. Niemelä, P. Pietiläinen, P. Hyvönen, and T. Chakraborty, *Europhys. Lett.* **36**, 533 (1996).
 - ³⁵ L. G. G. V. Dias da Silva, S. E. Ulloa, and A. O. Govorov, *Phys. Rev. B* **70**, 155318 (2004).
 - ³⁶ M. Grochol and R. Zimmermann, *Phys. Rev. B* **76**, 195326 (2007).
 - ³⁷ M. H. Degani, M. Z. Maijale, G. Medeiros-Ribeiro, and E. Ribeiro, *Phys. Rev. B* **78**, 075322 (2008).
 - ³⁸ See, e.g., Chap. 4 of H. Haug and S. W. Koch, *Quantum Theory of the Optical and Electronic Properties of Semiconductors*, Fifth Edition (World Scientific, Singapore, 2009), or Chap. 9 of P. Y. Yu and M. Cardona, *Fundamentals of Semiconductors*, Fourth Edition (Springer, Berlin, 2010).
 - ³⁹ \mathbf{r} in the Bloch functions (and integral of $\int^{(3D)}$) is a three-dimensional vector, describing the scale of lattice constant. In the other places, \mathbf{r} is a two-dimensional vector for the larger scale.
 - ⁴⁰ The basis functions are analytically obtained for the holes. Those for electrons are expressed as a linear combination of the eigenfunctions of $H_{e,0} = (\mathbf{p} + e\mathbf{A})^2 / (2m_e) + m_e \omega_c^2 r^2 / 2$, the coefficients of which are numerically determined.
 - ⁴¹ For example, the dimension is 4,339 for the states of three electrons with $L = 0$ and $S_{e,z} = 1/2$, and that is 5,339 for the states of trion with $L = 0$, $S_{e,z} = 0$, and $S_{h,z} = 1/2$.
 - ⁴² L. V. Keldysh, O. V. Konstantinov, and V. I. Perel', *Fiz. Tekh. Poluprovodn.* **3**, 1042 (1969), [*Sov. Phys. Semicond.* **3**, 876 (1970)].
 - ⁴³ B. P. Zakharchenya, D. N. Mirlin, V. I. Perel', and I. I. Reshina, *Usp. Fiz. Nauk.* **136**, 459 (1982), [*Sov. Phys. Usp.* **25**, 143 (1982)].
 - ⁴⁴ L. E. Ballentine, *Quantum Mechanics: A Modern Development* (World Scientific, Singapore, 1998).
 - ⁴⁵ M. Koskinen, M. Manninen, B. Mottelson, and S. M. Reimann, *Phys. Rev. B* **63**, 205323 (2001).
 - ⁴⁶ P. Koskinen, M. Koskinen, and M. Manninen, *Eur. Phys. J. B* **28**, 483 (2002).
 - ⁴⁷ Y. M. Liu, C. G. Bao, and T. Y. Shi, *Phys. Rev. B* **73**, 113313 (2006).
 - ⁴⁸ W. Heitler and F. London, *Z. Phys.* **44**, 455 (1927).